Received: 14 June 2020 | Revised: 29 July 2020 | Accepted: 8 September 2020

DOI: 10.1049/ote2.12011

IET Optoelectronics

The Institution of Engineering and Technology WILEY

ORIGINAL RESEARCH PAPER

Compensation for the non-uniformity correction of multi-channel TDI CCD under variable gain

Yun-Hui Li[1] | Xiao-Dong Wang[1] | Zhi Wang[1,2]

[1]Changchun Institute of Optics, Fine Mechanics and Physics, Chinese Academy of Sciences, Changchun, China

[2]Changchun UP Optotech (Holding) Co., Ltd., Changchun, China

Correspondence

Yun-Hui Li, Changchun Institute of Optics, Fine Mechanics and Physics, Chinese Academy of Sciences, No. 3888 Dong Nanhu Road, Changchun, China.

Email: liyunhui_ciomp@126.com

Funding information

Chinese Academy of Sciences, Grant/Award Number: XDA17010205

Abstract

The compensation for non-uniformity correction of multi-channel time delay integration charge coupled device (TDI CCD) under variable gain is presented. The mathematical model of photoelectric conversion is established first, and, then, a two-step non-uniformity correction method for multi-channel TDI CCD is proposed. Based on this method, a compensation algorithm for non-uniformity correction under variable gain is elaborated in detail. The experimental results show that the proposed algorithm can always maintain the photo response non-uniformity (PRNU) of the corrected images better than 1.14% when the programmable gain amplification (PGA) gain varies within the range of 1–3, compared to the conventional method of degrading to 2.91%. Meanwhile, a compression method for correction coefficients under multiple integral stages is proposed, which can reduce the storage space requirement by 50% at the cost of the PRNU being degraded by a maximum of 0.19% at all integral stages.

1 | INTRODUCTION

In recent years, with the gradual development of Earth remote sensing, astronomical observation, lunar remote sensing and deep space exploration missions, higher demands have been put forward for space optical imaging payloads. As a detector which is used widely in remote sensing field because of its high sensitivity and high signal-to-noise ratio (SNR), TDI CCD and its signal processing path are the core of photoelectric conversion in the imaging system, which directly affects the key performance of the system [1–3].

To achieve both wide-width and high-resolution imaging, the resolution requirement of the detector is gradually improved, which is difficult to meet through a single detector [4]. Therefore, optical splicing or mechanical splicing based on multiple detectors is commonly used in remote sensing systems. Meanwhile, to improve the imaging adaptability under different orbital parameters, the requirement of data readout rate is also gradually increased. Therefore, multi-channel bidirectional or unidirectional parallel readout mode is generally employed in the detector to improve pixel readout efficiency and suppress readout noise [5,6]. Based on the above situation, whether it is the performance difference between detectors, or the difference in signal processing between channels in the detector, or the difference in response characteristics of each pixel in the channel will result in response non-uniformity of the entire imaging focal plane, which needs to take effective measures for correction.

As an effective measure to make up for the errors of detector manufacturing and signal processing, non-uniformity correction is the key technology to improve the imaging quality. The development of non-uniformity correction technology is relatively mature, which mainly includes two kinds of methods: one is based on radiometric calibration and another is based on target scene.

The former method relies on the radiometric calibration experiment carried out in the laboratory or in orbit, which has the advantages of high precision, simple algorithm and good feasibility. However, periodic calibration is required with the aid of the calibration environment in the laboratory or the calibration light source in orbit to cope with the performance changes caused by the system ageing. Such methods include single-point correction, two-point correction, multi-point linear fitting correction, which are for linear response [7–14], and piecewise linear fitting correction, polynomial fitting correction, which are for nonlinear response [15–17].

The latter method is based on the real-time imaging scene to estimate the correction parameters, which has the advantage

of eliminating the calibration equipment and environment because there is no need for calibration, so it has better applicability. However, the algorithm is complex, and both the real-time performance and the precision need to be improved. This kind of method is mainly used in the Infrared Focal Plane Array (IRFPA) imaging system [18–20].

The methods based on radiometric calibration are more mature and therefore more widely used. Liu and Hao [9] discussed several non-uniformity correction methods, including single-point correction, two-point correction and multi-point correction, and the two-point correction method was finally adopted based on the linear response of TDI CCD. Considering the non-linear response of IRFPA, Sheng et al. analysed two-point correction, piecewise linear correction and polynomial fitting correction, and implemented the polynomial fitting method based on field programmable gate array (FPGA) hardware platform [17]. A pixel-wise linear radiance to digital conversion model was constructed by Yang et al. for crime scene imaging complementary metal oxide semiconductor (CMOS), and then pixel-wise conversion gain is calculated to correct Fixed Pattern Noise (FPN) [10]. Jin et al. [11] proposed a three-step non-uniformity correction algorithm based on the photoelectrical response model of Intensified Charge Coupled Device (ICCD), in which two steps adopt the non-linear two-point correction based on the S-curve model, and the remaining step adopts the linear two-point correction. Marta de Lasarte focussed on the methodology designed for the radiometric calibration experiment and assessed the influence of the algorithm's variables on the quality of correction [21].

When the performance changes because of the system ageing, periodic on-orbit radiometric calibration is essential. Haichao Li et al. provided a radiometric calibration method without the flat fields, which can make full use of satellite control of yaw angle to ensure that linear CCDs imaging the same region of non-uniform scene. After the acquisition of the same region image, the high precision radiometric calibration results can be obtained based on the histogram matching method [22]. According to the characteristics of multi-CCD imaging systems, Tao et al. developed an algorithm based on scene matching with an aid of the strong correlation between every two adjacent images, which can effectively overcome the influence of non-linear response [23]. Zhang et al. [24] reported an on-orbit radiometric calibration method that uses daytime data to estimate the calibration coefficients for the nighttime sensor in the LuoJia1-01.

In the research of non-uniformity correction for multi-channel and multi-CCD imaging systems, Zhai et al. [12] presented a synthetical correction algorithm for multi-TDI CCD camera, in which a two-point correction is applied within the channel, gain average correction is applied between channels, and scene-adaptive correction is applied between TDI CCDs. A real-time non-uniformity correction system was introduced by Yan Wang for a sort of large-area full-frame transfer CCD. In the procedure of correction, the non-uniformity between channels is corrected first, and, then, the non-uniformity between pixels is corrected [13]. Similar to Ref. 12, Zhu et al. [14] designed a novel correction algorithm, wherein a two-point correction is used within the channel, compensation gain is used for correction between channels, and compensation offset is used for correction between TDI CCDs.

To cope with the adjustment of on-orbit operating parameters, Yong-hui proposed an algorithm that can correct the photo response non-uniformity (PRNU) between channels and the pixels within the channel under different gains, offsets and integrated time [25]. A two-dimensional calibration technique was proposed by Chen et al. to correct the spatial non-uniformity in infrared imaging systems adapting to different integration time and time-varying offset with only one-time calibration [26].

With the orderly development of deep space exploration missions around the world, the environment and tasks faced by optical imaging payloads have become more complex and diverse. In practical applications, it is inevitable that the signal gain will be adjusted over a wide range to meet different imaging requirements. However, there is still lack of effective analysis for the influence of gain variation on the non-uniformity correction, and the compensation for non-uniformity correction coefficients under variable gain in the case of multi-channel parallel output also needs to be further studied, both of which are the key to be solved.

From the perspective of photoelectric signal processing path, the mathematical model of photoelectric conversion is established, and, then, a two-step non-uniformity correction method for multi-channel TDI CCD is proposed, which is consistent with the conventional method in the correction effect. On the basis of this method, a compensation method for non-uniformity correction under variable gain is proposed. By sequentially compensating the offset and gain of each channel and the digital correction coefficients of each pixel, the uniformity of the corrected images under different gains can be guaranteed. Meanwhile, with the goal of reducing the storage space requirement of correction coefficients, a compression method for coefficients under multiple integral stages is proposed, which can significantly reduce the amount of data that needs to be stored on-board.

The remainder is organised as follows: Section 2 describes the photoelectric signal processing path based on TDI CCD detector and specifically defines the hardware architecture. Then, the mathematical model is extracted from it. Section 3 presents the two-step non-uniformity correction method. Based on Section 3, the compensation method for non-uniformity correction parameters under variable gain is elaborated in Section 4. In Section 5, the compression method for correction coefficients is given. The experimental results and analysis of all the above methods are presented in Section 6. The conclusions are drawn in Section 7.

2 | PATH OF PHOTOELECTRIC SIGNAL PROCESSING

The general path diagram of photoelectric signal processing based on the CCD detector is shown in Figure 1. First of all, as the core of photoelectric conversion, CCD detector transforms

the incident light signal into an electronic charge packet, which is then converted to an analogue electrical signal through the CCD on-chip readout circuit. The analogue signal is sequentially subjected to the pre-amplification circuit to complete impedance matching and amplitude adjustment, the correlated double sampling (CDS) circuit to eliminate reset noise, the programmable gain amplification (PGA) circuit to adjust analogue signal gain, and, finally, the analogue-to-digital conversion (ADC) circuit to complete analogue-to-digital quantisation conversion, in which the CCD output signal level in the dark field is adjusted by the analogue offset. The digital signal output by ADC circuit is pre-processed in real time (including non-uniformity correction, etc.) to get the final digital image.

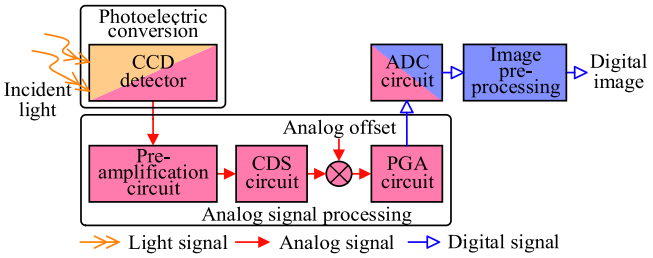

FIGURE 1 Path of photoelectric signal processing based on charge coupled device (CCD) detector

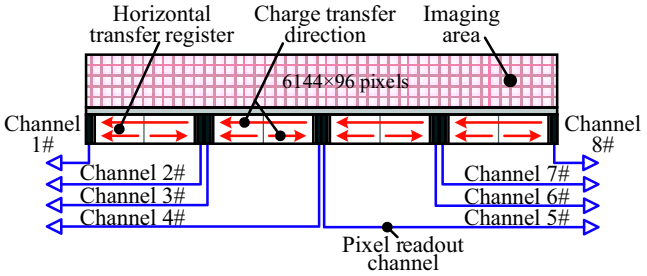

FIGURE 2 Architecture of time delay integration charge coupled device (TDI CCD) detector

A multi-spectral TDI CCD is used in our design to capture both panchromatic and multi-spectral images simultaneously. The non-uniformity correction method proposed takes the panchromatic image as an example for analysis, and the architecture of panchromatic part on the detector is shown in Figure 2. The number of effective pixels in the panchromatic part is 6144 with a maximum of 96 integral stages. The pixel readout adopts four-channel unidirectional transfer readout mode or eight-channel bidirectional transfer readout mode, which can be switched by modifying the driving signal timing. To achieve a higher push-scan frequency in the case of a lower pixel clock to reduce the readout noise, the eight-channel bidirectional readout operation is undoubtedly a better choice.

The specific processing path design for the signal originating from the TDI CCD detector is shown in Figure 3. The CCD on-chip readout circuit is a two-and-half stage amplifier, which requires a relatively complex external current source as the output load, and it is replaced with a resistor to simplify the design. The analogue front-end pre-amplification circuit adopts a structure of in-phase proportional amplification, and the gain G_1 is related to the value of its peripheral resistors, which can be expressed as

$$G_1 = \frac{R_2 \cdot (R_3 + R_4)}{(R_1 + R_2) \cdot R_3} \tag{1}$$

The dedicated video processor LM98640 integrated with CDS circuit, PGA circuit and ADC circuit is used for the

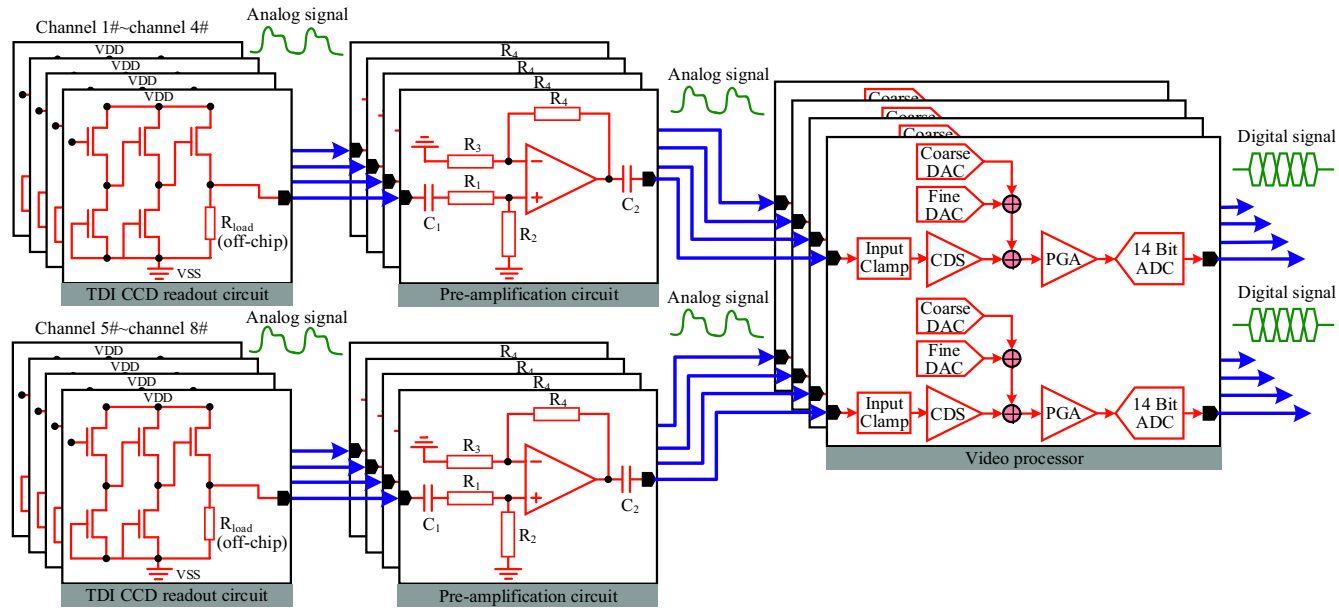

FIGURE 3 Design of photoelectric signal processing path based on time delay integration charge coupled device (TDI CCD) detector

conversion of the analogue signal output from pre-amplification circuit to the digital image, and its internal functional architecture is shown in Figure 3 [27]. The analogue signal input to the video processor first sets the reference level by clamp module, and then the difference between reference level and signal level is collected by CDS module, followed by offset module, PGA module and ADC module, wherein the offset is completed by a combination of coarse and fine digital-to-analogue conversion (DAC) circuit. The output digital image is then transmitted to the FPGA controller and real-time non-uniformity correction is implemented within it.

For the panchromatic part of the selected CCD, a total of eight pre-amplification circuits and four video processors due to two identical processing modules inside each processor are required to complete the signal acquisition, processing and quantisation.

A mathematical model is established by abstracting the hardware architecture described above. In the whole signal processing path of converting light signal to digital image, there are four typical signal adjustments, which are the photoelectric response of detector, the pre-amplification circuit, the offset circuit and the PGA circuit. The photoelectric response characteristic of TDI CCD detector can be expressed as follows:

$$S_A = \sum_{j=1}^{m} \left(\int_{\lambda 1}^{\lambda_2} R_j(\lambda) \cdot E(\lambda) \cdot T \cdot d\lambda \right) + V_d + \delta \tag{2}$$

where $E(\lambda)$ represents the spectral irradiance and $R_j(\lambda)$ represents the spectral responsivity of the jth pixel in the m-integral stage with a spectral range of λ_1 to λ_2. T is the line exposure time, which is equal to the reciprocal of the line frequency. V_d and δ are dark signal and noise, respectively, and S_A is the analogue signal output by the detector. Compared with conventional linear CCD, TDI CCD employs an operation mode called time delay integration, so that the actual response output is a superposition of m pixels in the m-integral stage.

Assuming that the pre-amplification circuit has a gain of G_1, the offset is set to B_2, and the PGA gain is set to K_2 inside the video processor, then, the transfer characteristic from the analogue signal output by CCD to the digital signal is:

$$D = \frac{K_2 \cdot (G_1 \cdot S_A + B_2)}{\mathrm{V_{REF}}} \times 2^b = K_2 \cdot (G_1 \cdot S_A + B_2) \cdot C \tag{3}$$

where D represents the grey value of the output digital image, $\mathrm{V_{REF}}$ and b are the reference voltage and the quantisation depth of the ADC circuit, respectively, and $2^b/\mathrm{V_{REF}}$ is recorded as constant C for convenience.

In practical applications, the pre-amplification circuit gain depends on the value of its peripheral resistors, which is inconvenient to modify after the system hardware is completes. To adapt to different irradiation environments, there are two ways to adjust the signal gain. One is to change the integral stages by modifying the driving timing to achieve rough adjustment, and the other is to change the PGA gain by modifying the register settings of the video processor to achieve fine adjustment.

3 | NON-UNIFORMITY CORRECTION METHOD WITH TWO STEPS

For the imaging focal plane composed of multi-TDI CCD detectors, which is widely used in wide field of view and high-resolution imaging systems, the non-uniformity of response is manifested in three aspects: the non-uniformity between detectors, the non-uniformity between internal channels of the detector and the non-uniformity between internal pixels of the channel, of which the first two can be unified as the non-uniformity between channels according to the processing method.

The correction method described here is carried out in two steps, aiming at the non-uniformity of the above two aspects. The first step is to adjust the analogue signal by setting the offset and PGA gain to achieve the non-uniformity correction between channels. On the basis of this, the second step is to adjust the digital signal by the pre-stored correction coefficients to achieve the non-uniformity correction between pixels within the channel.

3.1 | Step 1: Correction between channels

The discreteness of performance between detectors, the difference of pixel readout circuit between channels within the detector and the electrical parameter errors in the signal processing path all contribute to the difference in response characteristics between channels. Offset and PGA gain adjustment are effective means to make up for these differences, and they can be achieved simply by setting registers in the video processor. The calculation method of the parameters to be adjusted is derived as follows.

Since the photoelectric response of the TDI CCD is approximately linear, in a specific spectral range, its response characteristic can be simplified as follows:

$$S_A = R \cdot E \cdot T + \xi = R \cdot H + \xi \tag{4}$$

where R is the equivalent average spectral responsivity within the spectral range after a superposition of m pixels in the m-integral stage and H is the irradiation, which is the product of the average spectral irradiance E and the line exposure time T. ξ is the output offset that covers dark signal and noise.

It is assumed that the pre-amplification circuit of channel p has an actual gain of G_{1p} because of errors, and the offset and PGA gain are set to B_2 and K_2, respectively. Based on the above simplification, the average response characteristic of channel p can be expressed as

$$\overline{D}_p = K_2 \cdot \left[G_{1p} \cdot \left(\overline{R}_p \cdot H + \overline{\xi}_p \right) + B_2 \right] \cdot C \tag{5}$$

where $\overline{\mathbf{R}}_p$ and $\overline{\boldsymbol{\xi}}_p$ represent the average spectral responsivity and the average offset of all pixels in the channel, respectively, and the average grey value of the image acquired by the channel is $\overline{\mathbf{D}}_p$.

Adjusting the offset and PGA gain to B'_{2p} and K'_{2p}, respectively, so that the average response characteristic of channel p is consistent with the average response characteristic of the entire detector, namely:

$$\overline{D} = K'_{2p} \cdot \left[G_{1p} \cdot \left(\overline{R}_p \cdot H + \overline{\xi}_p \right) + B'_{2p} \right] \cdot C \tag{6}$$

where $\overline{\mathbf{D}}$ is the average grey value of the image acquired by the entire detector.

Getting K'_{2p} and B'_{2p} is the key to complete the correction between channels, and the necessary parameters for solving them need to be obtained by radiometric calibration experiments. The calibration process is to acquire a sequence of images with different irradiances under the condition of uniform irradiation. Linear fitting is then performed based on the average grey value of the image acquired by channel p as the independent variable, and the average grey value of the image acquired by all channels as the dependent variable. The slope W_p and the intercept Z_p of the fitted curve will satisfy the following relationship:

$$W_p \cdot \overline{D}_p + Z_p = \overline{D} \tag{7}$$

By combining Equations (5), (6) and (7), we can get

$$\begin{cases} K'_{2p} = W_p \cdot K_2 \\ B'_{2p} = \dfrac{1}{K_2 \cdot C} \cdot \dfrac{Z_p}{W_p} + B_2 \end{cases} \tag{8}$$

Then, the register settings of the video processor are modified according to the above results to complete the first step correction.

3.2 | Step 2: Correction between pixels within the channel

Constrained by the manufacturing process, there are inevitably physical deviations for each pixel in the detector, which will lead to differences in the dark signal and responsivity. These differences need to be digitally corrected by pre-stored coefficients, which is consistent with the traditional correction method.

The grey value of the output image is corrected by the correction coefficients $M_{p,q}$ and $N_{p,q}$, so that the response characteristic of each pixel in channel p can be consistent with the average response characteristic of the entire detector, so there is

$$\overline{D} = M_{p,q} \cdot D_{p,q} + N_{p,q} \tag{9}$$

where $D_{p,q}$ is the grey value of the qth pixel in channel p.

On the basis of the first step correction, the correction coefficients $M_{p,q}$ and $N_{p,q}$ need to be obtained by the second radiometric calibration experiment. Similar to the first radiometric calibration experiment, the second calibration process is to acquire a sequence of images with different irradiances under the condition of uniform irradiation. Linear fitting is then performed based on the grey value of the qth pixel in channel p as the independent variable, and the average grey value of the image acquired by all channels as the dependent variable. The slope and the intercept of the fitted curve will correspond to the coefficients $M_{p,q}$ and $N_{p,q}$, respectively.

Then, the obtained correction coefficients are pre-stored in the non-volatile memory on-board, and the real-time non-uniformity correction is realised by reading the coefficients and correcting the output grey value according to Equation (9).

4 | COMPENSATION FOR CORRECTION COEFFICIENTS UNDER VARIABLE GAIN

4.1 | Step 1: Compensation between channels

According to the control instructions, it may be necessary to change the offset and PGA gain to B_3 and K_3, respectively, to meet the imaging requirements under different environmental conditions, at which, the average response characteristic of channel p can be expressed as

$$\overline{D}'_p = K_3 \cdot \left[G_{1p} \cdot \left(\overline{R}_p \cdot H + \overline{\xi}_p \right) + B_3 \right] \cdot C \tag{10}$$

The above equation needs to be solved with the help of Equation (6), which represents the response characteristic of channel p adjusted by B'_{2p} and K'_{2p}, and it is consistent with the average response characteristic of the entire detector. Therefore, $K'_{2p} \cdot C \cdot G_{1p} \cdot \overline{R}_p$ is denoted as $\overline{\boldsymbol{\lambda}}$, and $K'_{2p} \cdot C \cdot (G_{1p} \cdot \overline{\xi}_p + B'_{2p})$is denoted as $\overline{\mathbf{e}}$ in the equation, both of which are constants independent of channel p, and then they are substituted into Equation (10) to get

$$\overline{D}'_p = \frac{K_3}{K'_{2p}} \cdot \overline{\lambda} \cdot H + \frac{K_3}{K'_{2p}} \cdot \overline{e} + K_3 \cdot C \cdot \left(B_3 - B'_{2p} \right) \tag{11}$$

To ensure that the average response characteristic of channel p remains consistent with the average response characteristic of the entire detector after the parameters change, the offset and PGA gain of channel p need to be adjusted as follows:

$$\begin{cases} K_{3p}^{'} = \dfrac{K_{2p}^{'}}{K_2} \cdot K_3 \\ B_{3p}^{'} = B_{2p}^{'} + \theta \end{cases} \tag{12}$$

where B'_{3p} and K'_{3p} are the results after the parameters change and need to be updated to the video processor. θ is a constant that can be set to any value as required.

Replace B_3 and K_3 in Equation (11) with the above results B'_{3p} and K'_{3p}, and, then, we can get the average response characteristic of the entire detector under variable gain as follows:

$$\overline{D}^{'} = \frac{K_3}{K_2} \cdot \overline{\lambda} \cdot H + \frac{K_3}{K_2} \cdot \overline{e} + K_3 \cdot C \cdot \theta \tag{13}$$

4.2 | Step 2: Compensation between pixels within the channel

Before changing the offset and PGA gain, the qth pixel in channel p is first corrected by the offset and PGA gain B'_{2p} and K'_{2p} and then corrected by the coefficients $M_{p,q}$ and $N_{p,q}$ to achieve the same response characteristic as the entire detector, namely:

$$\overline{D} = M_{p,q} \cdot \left\{ K_{2p}^{'} \cdot \left[G_{1p} \cdot \left(R_{p,q} \cdot H + \xi_{p,q} \right) + B_{2p}^{'} \right] \cdot C \right\} + N_{p,q} \tag{14}$$

where $R_{p,q}$ and $\xi_{p,q}$ represent the spectral responsivity and the offset of the qth pixel in channel p, respectively.

After changing the offset and the PGA gain, the qth pixel in channel p is also first corrected by the adjusted offset and PGA gain B'_{3p} and K'_{3p} and then corrected by the adjusted coefficients $M'_{p,q}$ and $N'_{p,q}$ to maintain its response characteristic consistent with the entire detector, namely:

$$\overline{D}^{'} = M_{p,q}^{'} \cdot \left\{ K_{3p}^{'} \cdot \left[G_{1p} \cdot \left(R_{p,q} \cdot H + \xi_{p,q} \right) + B_{3p}^{'} \right] \cdot C \right\} + N_{p,q}^{'} \tag{15}$$

By combining Equations (13), (14), (15) and (6), we can get

$$\begin{cases} M_{p,q}^{'} = M_{p,q} \\ N_{p,q}^{'} = \dfrac{K_3}{K_2} \cdot N_{p,q} + K_3 \cdot C \cdot \theta \cdot \left(1 - M_{p,q} \cdot \dfrac{K_{2p}^{'}}{K_2} \right) \end{cases} \tag{16}$$

According to the above derivation process, the compensation for non-uniformity correction under variable gain can be divided into two steps:

1. When the offset and the PGA gain need to be changed to B_3 and K_3 based on the control instructions, the adjusted offset and the PGA gain B'_{3p} and K'_{3p} of each channel should be calculated according to Equation (12) first, and then updated to the corresponding video processors.
2. The pre-stored original correction coefficients $M_{p,q}$ and $N_{p,q}$ are read out and substituted into Equation (16) to calculate the adjusted correction coefficients $M'_{p,q}$ and $N'_{p,q}$, which will be used as the coefficients of the qth pixel in channel p for correction.

5 | COMPRESSION FOR CORRECTION COEFFICIENTS

Based on its special operation mode of time delay integration, the response output of the TDI CCD is a superposition of m pixels in the m-integral stage, as shown in Equation (2) above. For TDI CCD detectors that are used in the field of space remote sensing, the integral stages can usually be changed by modifying the driving timing to meet different environmental conditions. For example, the TDI CCD detector used in our design has 8-stage, 16-stage, 32-stage, 48-stage, 64-stage and 96-stage with a total of six variable stages.

As a kind of linear CCD, TDI CCD does not have the non-uniformity in the column direction originally, but the pixels participating in the integration will be different under various integral stages, and there are also differences in the response characteristic between pixels in the same column, so that the output response characteristics are not strictly proportional to the integral stage, which leads to the fact that the correction coefficients for one integral stage are not applicable to other integral stages.

The general solution to this problem is to perform radiometric calibration experiments separately at all integral stages, and a total of six sets of correction coefficients are pre-stored in the non-volatile memory on-board to cope with different integral stages, which is equivalent to six times the storage space requirement compared to the conventional linear CCD.

With the goal of reducing the storage space requirement of correction coefficients, a compression method for coefficients under multiple integral stages of a single pixel is proposed. The basic principle is to find a polynomial that can express these coefficients, and then store the coefficients of the polynomial instead of correction coefficients, so as to significantly reduce the storage space requirement.

For the panchromatic part of TDI CCD used in our design, the correction coefficients of the qth pixel in channel p under various integral stages are expressed as $M_{p,q}^{i}$ and $N_{p,q}^{i}$, where i represents the index of integral stage, and its range from 1 to 6 corresponds to six integral stages, respectively. Then take the coefficient $M_{p,q}^{i}$ as an example, it can be fitted by

a quadratic polynomial with the help of the least square method, and the fitting coefficients can be solved by the following equation:

$$\begin{bmatrix} \sum_{i=1}^{6} 1 & \sum_{i=1}^{6} G^i & \sum_{i=1}^{6} (G^i)^2 \\ \sum_{i=1}^{6} G^i & \sum_{i=1}^{6} (G^i)^2 & \sum_{i=1}^{6} (G^i)^3 \\ \sum_{i=1}^{6} (G^i)^2 & \sum_{i=1}^{6} (G^i)^3 & \sum_{i=1}^{6} (G^i)^4 \end{bmatrix} \begin{bmatrix} a_{p,q} \\ b_{p,q} \\ c_{p,q} \end{bmatrix} = \begin{bmatrix} \sum_{i=1}^{6} M_{p,q}^i \\ \sum_{i=1}^{6} G^i \cdot M_{p,q}^i \\ \sum_{i=1}^{6} (G^i)^2 \cdot M_{p,q}^i \end{bmatrix} \quad (17)$$

where matrix $G = [8\ 16\ 32\ 48\ 64\ 96]$, and i in G^i represents the index of the elements in the matrix.

In this way, only three coefficients $a_{p,q}$, $b_{p,q}$ and $c_{p,q}$ need to be stored for the qth pixel in channel p. When the non-uniformity correction is performed in orbit, $M^i_{p,q}$ is calculated by the following equation according to the current integral stage G^i:

$$M_{p,q}^i = a_{p,q} + b_{p,q} \cdot G^i + c_{p,q} \cdot (G^i)^2 \quad (18)$$

The same processing method is adopted for the coefficient $N^i_{p,q}$. Then, for a single pixel, this method reduces the number of coefficients from 12 to 6, that is, the storage space is reduced by 50%, and the more the number of variable stages is, the greater the advantage of storage space is. However, the proposed method increases the step of recovering the correction coefficients from the compressed data, which undoubtedly increases the amount of calculation. Moreover, the curve fitting error also leads to the error of restored coefficients, thereby having a certain impact on the effect of non-uniformity correction. The extent of this impact needs to be quantified by the following experiments.

6 | EXPERIMENTAL RESULTS AND ANALYSIS

6.1 | Experimental parameters and evaluation index

The experimental verification system is shown in Figure 4, which mainly consists of the imaging focal plane composed of a TDI CCD detector and its driving circuit and video processing circuit, the integrating sphere for generating uniform irradiation, the instruction computer for setting imaging parameters and the computer for acquiring image data. The experiment was carried out in a dark room to isolate external irradiation contamination.

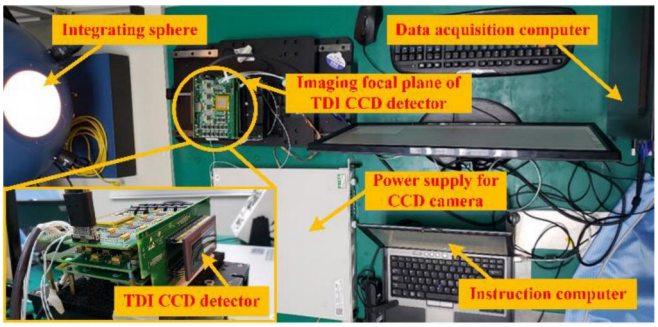

FIGURE 4 Construction of experimental verification system

The number of effective pixels in the panchromatic part of the selected detector is 6144 with a maximum of 96 integral stages. The 8-channel bidirectional readout operation mode is adopted in our design, and each channel is responsible for reading 768 pixels. Because some of the readout channels are damaged, only the effective output data from the last four channels that are in good condition are acquired and further analysed.

The load resistor R_{load} at the output of the detector is 1.5 kΩ; in this case, the detector's saturation response output is about 2100 mV. The pre-amplification circuit gain G_1 is set to 1 through its peripheral resistors, where R_1 to R_4 are all 620 Ω. The signal is alternating current (AC) coupled, and the coupling capacitance C_1 and C_2 are 0.1 uF. In the video processor, the offset B_2 and the PGA gain K_2 are initially set to 0 mV and 1, respectively. The reference voltage V_{REF} of the ADC circuit is 2 V, and the upper 12 bits of the 14-bit ADC output are taken as effective data.

The performance of the non-uniformity correction is evaluated by the PRNU index, which is generally defined as the ratio of the standard deviation to the average in terms of the grey value under the condition of semi-saturated uniform irradiation. The mathematical expression of PRNU is

$$\text{PRNU} = \frac{1}{\overline{D}} \cdot \sqrt{\frac{1}{P \cdot Q} \cdot \sum_{p=1}^{P} \sum_{q=1}^{Q} (D_{p,q} - \overline{D})^2} \quad (\text{Units}: \%) \quad (19)$$

where $D_{p,q}$ is the grey value of the qth pixel in channel p, and the detector has a total of P channels, each of which has Q effective pixels. $\overline{\mathbf{D}}$ represents the average grey value of all pixels.

6.2 | Results of non-uniformity correction with two steps

Under the premise of a fixed integral stage and line frequency, the conventional correction method is carried out first for comparison, that is, a sequence of images under different irradiances is acquired by the calibration experiment, and then the correction coefficients are calculated directly by multi-point

linear fitting based on the acquired images, and, finally, these coefficients are stored in the non-volatile memory on-board to complete the real-time correction according to Equation (9).

Then the two-step non-uniformity correction method proposed is carried out, that is, a sequence of images under different irradiances is acquired first, and then the adjusted offset and the PGA gain for each channel are calculated according to Equation (8), which will be updated to the video processor to complete the first step correction. On the basis of the first step, the same experimental content is carried out again, and the calculation and the storage of the correction coefficients are the same as the conventional method.

Figure 5 shows the images corrected by the conventional method and the proposed two-step method and their grey value distribution curves in the case of semi-saturated output. It can be seen from the figure that the proposed method can eliminate the obvious dividing line between channels only by the first step correction, and the second step can further eliminate the non-uniformity within the channel on the basis of the first step. Both methods can eventually achieve excellent correction results.

The PRNU values of the images corrected by the conventional method and our method under different average grey values are recorded in Table 1. It can be seen that in all cases, the non-uniformity of the images corrected by the two methods is basically consistent. Both methods can achieve a PSNR value of 0.27% in the case of semi-saturated output. Compared with the conventional correction method, the advantage of the two-step method is that its first step can significantly eliminate the imaging differences between channels by adjusting the register parameters, thereby achieving a significant reduction in non-uniformity. In other words, when the implementation resources for correction with digital coefficients are limited, a relatively acceptable result can be achieved just by the first step correction.

The probability density distributions of the correction coefficients for the two methods are shown in Figure 6. For the conventional correction method, in addition to correcting the difference in response between pixels, the correction coefficients also need to correct the difference of the signal processing circuits between channels, resulting in a relatively dispersed coefficient distribution. In contrast, since the first step of our method matches the response characteristics between channels, the correction coefficients in the second step are mainly responsible for correcting the difference in response between pixels, so the coefficient distribution is more centralised, which brings certain benefits to the possible data compression.

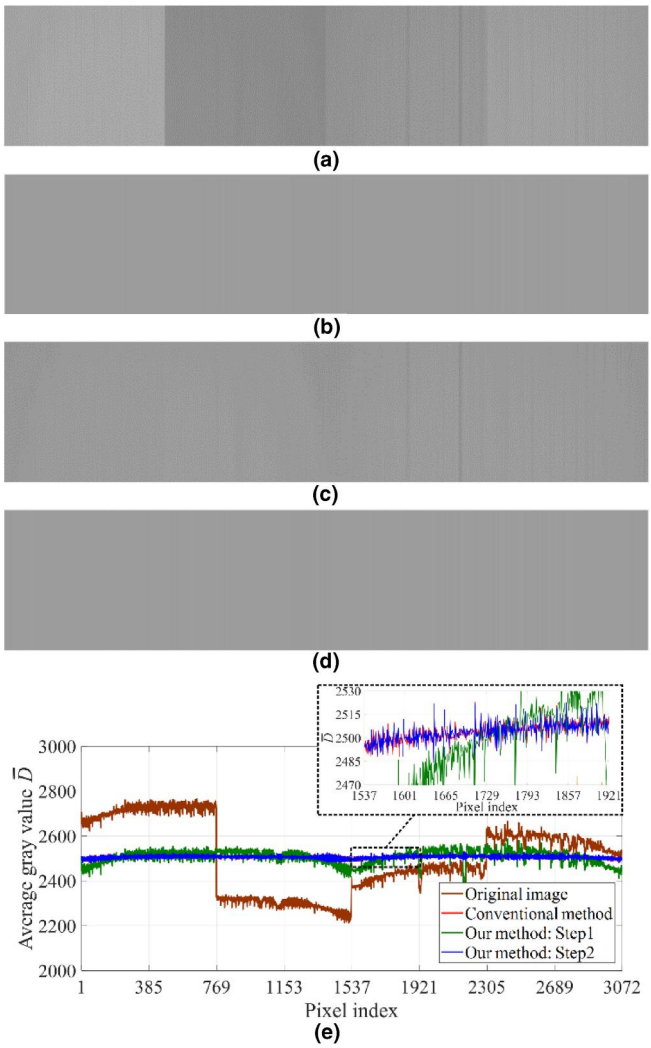

FIGURE 5 The corrected images in the case of semi-saturated output. (a) Original image, (b) the image corrected by the conventional method, (c) the image corrected only by the first step of the proposed two-step method, (d) the image corrected by both the two steps of the proposed two-step method and (e) comparison of grey value distribution curves obtained by different correction methods

TABLE 1 The PRNU values of the images corrected by different methods

Average grey value $\overline{D}$	643 (%)	1422 (%)	1905 (%)	2506 (%)
Original image	8.87	6.96	6.63	6.40
Our method: Step 1	1.74	1.06	1.17	1.19
Our method: Step 2	0.98	0.93	0.63	0.27
Conventional method	0.99	0.92	0.63	0.27

Abbreviation: PRNU, photo response non-uniformity.

6.3 | Results of compensation for coefficients under variable gain

Similarly, under the premise of a fixed integral stage and line frequency, the offset B_2 and the PGA gain K_2 are initialised to the default values of 0 mV and 1, respectively. When the PGA gain needs to be modified according to the imaging environment, as a comparison, the real-time correction process is first performed by the conventional method as described in Section 6.B without compensation.

Then, the radiometric calibration experiment is carried out by the proposed two-step method, and the calculation results are updated to the video processor and the non-volatile

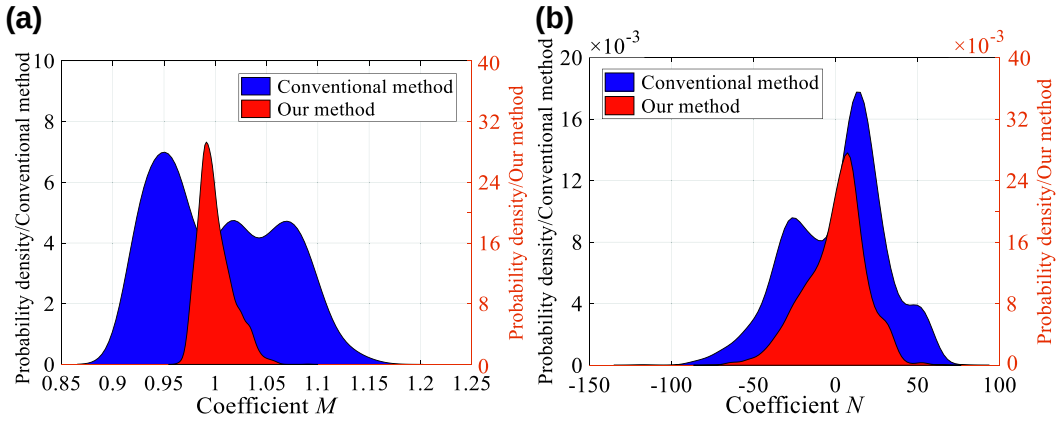

FIGURE 6 The probability density distributions of the correction coefficients. (a) Correction coefficient M and (b) correction coefficient N

memory, respectively. When the PGA gain needs to be modified according to the imaging environment, the compensated offset and the gain are first calculated according to Equation (12) and reloaded into the video processor, and then, the compensated correction coefficients are calculated according to Equation (16), which is finally used to complete the real-time non-uniformity correction.

When the PGA gain is modified to 1.6, the images are corrected by the conventional method and the proposed two-step compensation method, respectively, and their grey value distribution curves in the case of semi-saturated output are shown in Figure 7.

In the case of semi-saturated output, the PRNU values of the images corrected by the conventional method and our method under various modified gains are recorded in Table 2. It can be seen that the larger the modified gain, the more serious the non-uniformity of the original image. With the increase of the gain, the non-uniformity of the image corrected by the conventional method deteriorates significantly, while the non-uniformity of the image corrected by the proposed compensation method can always be maintained well. The larger the gain is, the more obvious the advantage of our method is. When the PGA gain varies within the range of 1–3, the proposed method can always maintain the PRNU of the corrected images better than 1.14%, compared to the conventional method of degrading to 2.91%.

In fact, there is no theoretical deviation in the proposed two-step compensation method, but when the gain increases, the detector's low irradiance response is used in the case of semi-saturated output. Due to the poor linearity at low irradiance, the uniformity will inevitably be degraded to some extent even after compensation. However, the overall performance is still significantly superior to the conventional method.

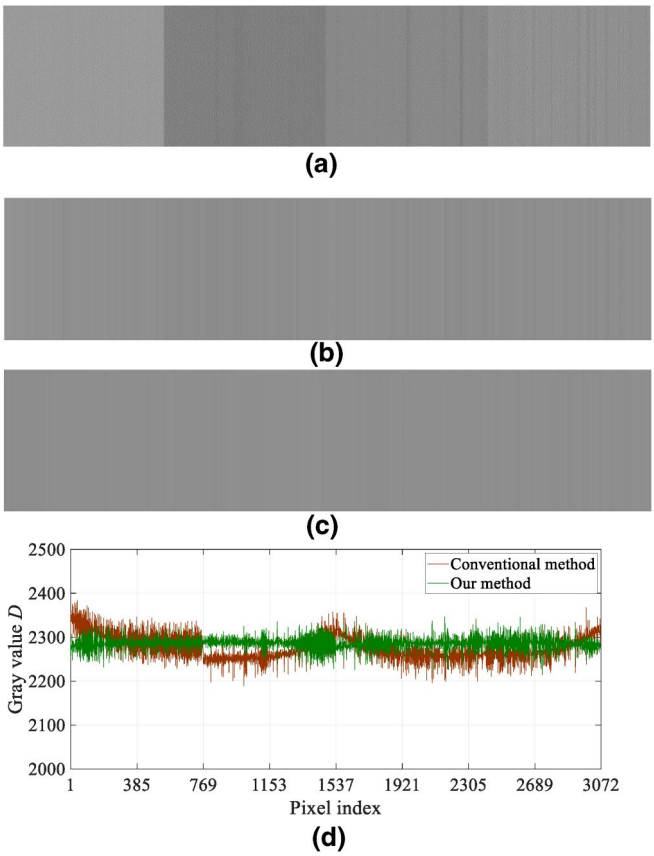

FIGURE 7 The corrected images in the case of semi-saturated output when the programmable gain amplification (PGA) gain is modified to 1.6. (a) Original image, (b) the image corrected by the conventional method, (c) the image corrected by the proposed two-step compensation method and (d) comparison of grey value distribution curves obtained by different correction methods

6.4 | Verification of compression for correction coefficients

First, the original correction coefficients under all integral stages are obtained by the radiometric calibration experiments, and then they are substituted into Equation (17) to obtain the fitting coefficients of each pixel, which need to be stored in the non-volatile memory on-board. When the non-uniformity correction is performed in orbit, the restored coefficients for real-time correction are calculated by Equation (18) according to the current integral stage.

TABLE 2 The PRNU values of the images corrected by different methods under various modified gains

PGA gain	Original image (%)	Conventional method (%)	Our method: Step 1 (%)	Our method: Step 2 (%)
$K_3 = 1.0$	6.40	0.27	1.19	0.27
$K_3 = 1.2$	6.63	0.69	1.17	0.64
$K_3 = 1.6$	6.95	1.29	1.17	0.70
$K_3 = 3.0$	8.87	2.91	1.76	1.14

Abbreviations: PGA, programmable gain amplification; PRNU, photo response non-uniformity.

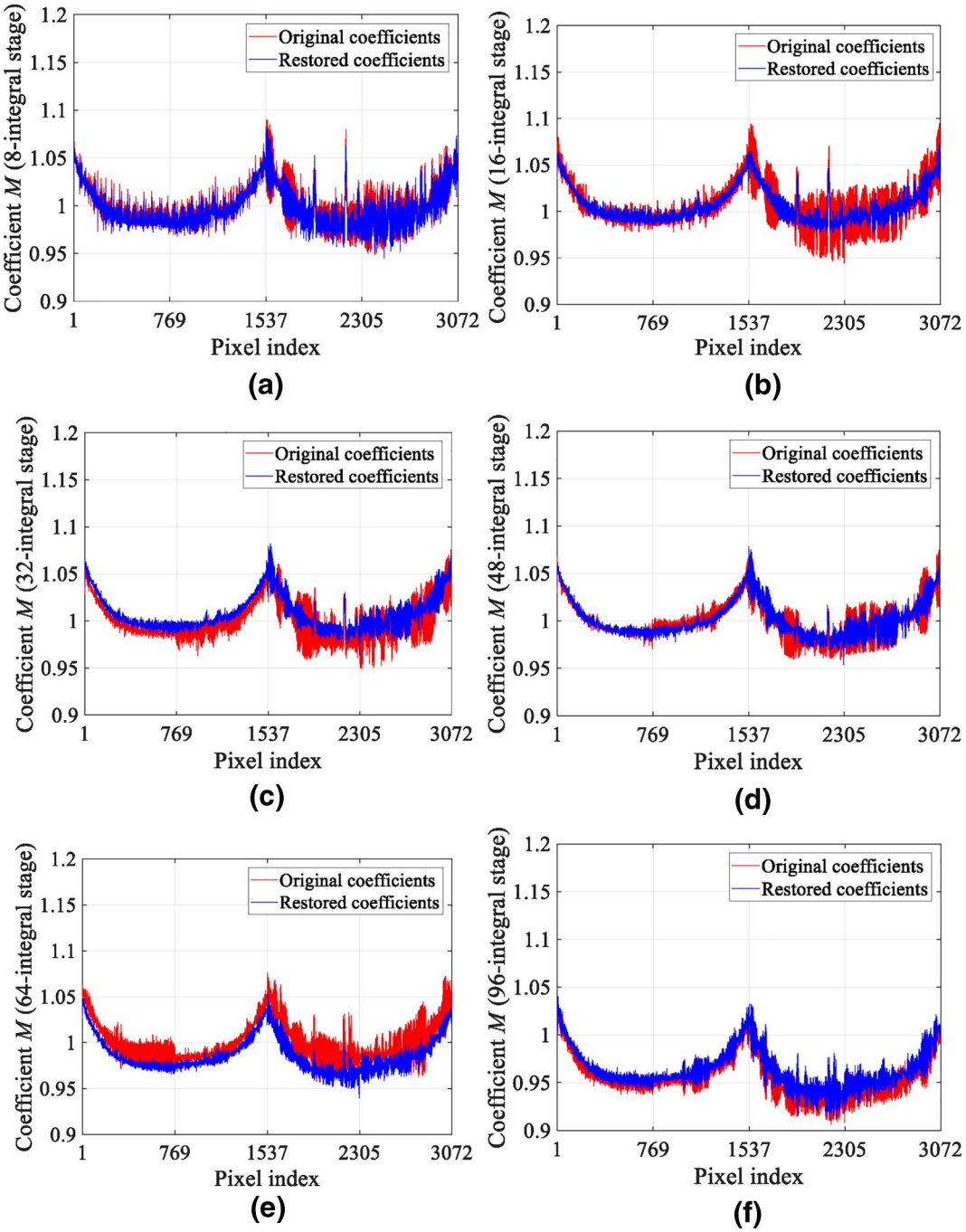

FIGURE 8 Comparison between the original and the restored correction coefficients $M^{i}_{p,q}$ under different integral stages. (a) 8-integral stage, (b) 16-integral stage, (c) 32-integral stage, (d) 48-integral stage, (e) 64-integral stage and (f) 96-integral stage

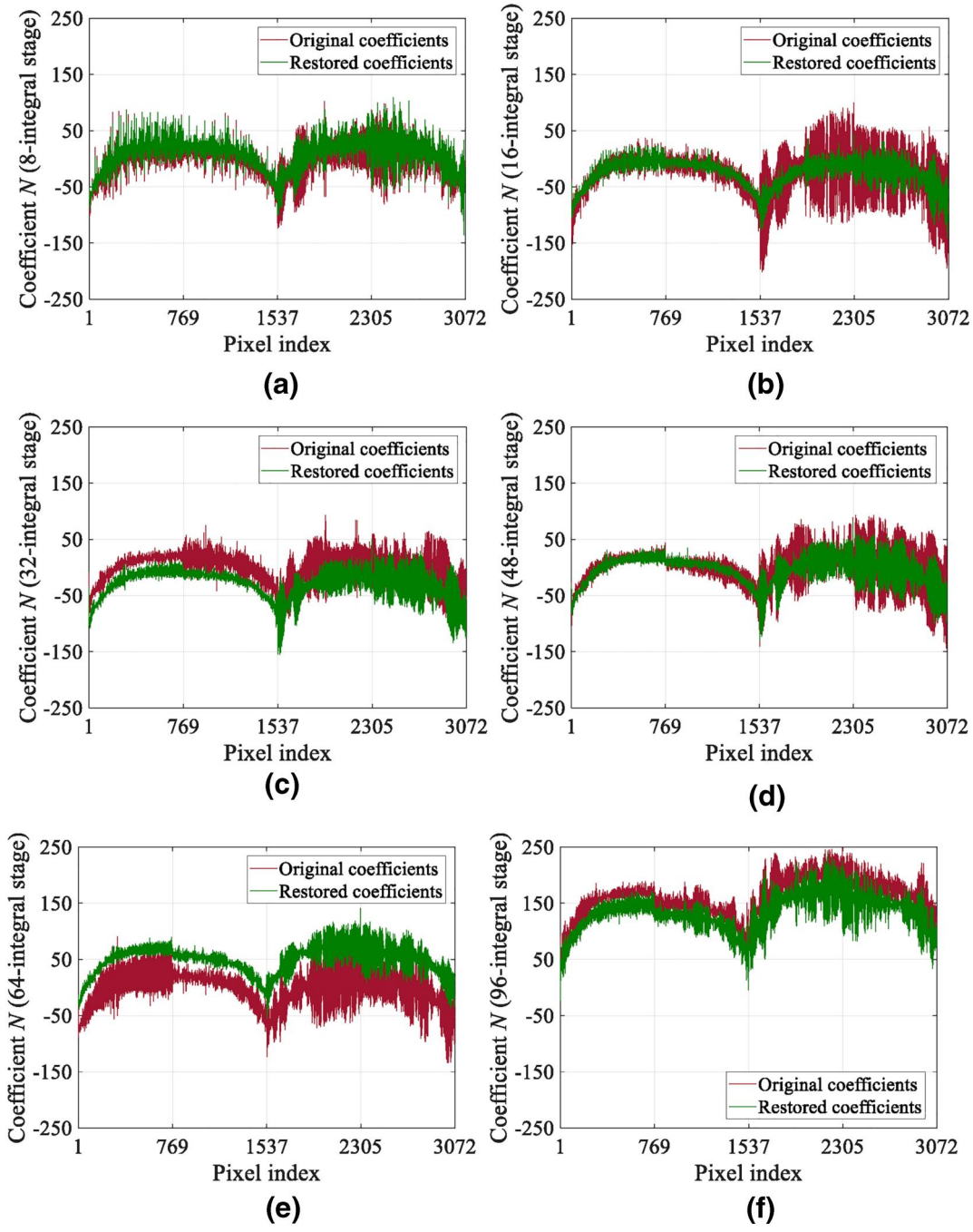

FIGURE 9 Comparison between the original and the restored correction coefficients $N^{i}_{p,q}$ under different integral stages. (a) 8-integral stage, (b) 16-integral stage, (c) 32-integral stage, (d) 48-integral stage, (e) 64-integral stage and (f) 96-integral stage

Figures 8 and 9 show the comparison between the original correction coefficients and the restored correction coefficients under different integral stages, wherein Figure 8 corresponds to the correction coefficient $M^{i}_{p,q}$, and Figure 9 corresponds to the correction coefficient $N^{i}_{p,q}$. It can be seen that there are some small differences between the two sets of coefficients, but they can basically be consistent in general.

Under different integral stages, the PRNU values of the images corrected by the original coefficients and the restored coefficients, respectively, are recorded in Table 3. It can be seen that the uniformity of the images corrected by the latter has a slight degradation, which is acceptable to some extent for the application of limited resources on-board. The proposed method can reduce the number of coefficients from 12 to 6 for a single pixel, that is, the storage space is reduced by 50% at the cost of the PRNU of the corrected images being degraded by a maximum of 0.19% at all integral stages.

TABLE 3 The PRNU values of the images corrected by the original coefficients and the restored coefficients under different integral stages

Integral stage	Original image without correction (%)	Corrected by original coefficients (%)	Corrected by restored coefficients (%)	Difference between the previous two columns (%)
8	6.55	0.63	0.62	−0.01
16	6.45	0.51	0.59	+0.08
32	6.47	0.62	0.71	+0.09
48	6.40	0.64	0.78	+0.14
64	6.38	0.43	0.62	+0.19
96	6.28	0.51	0.56	+0.05

Abbreviation: PRNU, photo response non-uniformity.

7 | CONCLUSIONS

In the face of increasingly complex and diverse imaging environment, the compensation for non-uniformity correction of multi-channel TDI CCD under variable gain is presented.

First, a two-step non-uniformity correction method for multi-channel TDI CCD is proposed, which is consistent with the conventional method in the correction effect. The advantage of the proposed method is that its first step can significantly eliminate the imaging differences between channels by adjusting the register parameters, thereby achieving a significant reduction in non-uniformity. In other words, when the implementation resources for correction with digital coefficients are limited, a relatively acceptable result can be achieved just by the first step correction. Moreover, in contrast, the coefficient distribution is more centralised, which brings certain benefits to the possible data compression.

Second, on the basis of the above method, a compensation method for non-uniformity correction under variable gain is proposed. By sequentially compensating the offset and gain of each channel and the digital correction coefficients of each pixel, the uniformity of the corrected images under different gains can be guaranteed. The experimental results based on the verification system show that the compensation method can always maintain the PRNU of the corrected images better than 1.14% when the PGA gain varies within the range of 1–3, compared to the conventional method of degrading to 2.91%.

Finally, with the goal of reducing the storage space requirement of correction coefficients, a compression method for coefficients under multiple integral stages is proposed. Under the verification system parameters, this method can reduce the number of coefficients from 12 to 6 for a single pixel, that is, the storage space is reduced by 50% at the cost of the PRNU of the corrected images being degraded by a maximum of 0.19% at all integral stages.

The methods proposed enhance the adaptability of optical remote sensing payloads in complex imaging environments while also improving the cost performance.

ACKNOWLEDGEMENTS

This work was supported by the Strategic Priority Research Program of Chinese Academy of Sciences (Grant No. XDA17010205).

REFERENCES

1. Wong, H.-S., Yao, Y.L., Schlig, E.S.: TDI charge-coupled devices: Design and applications. IBM J. Res. Dev. 36, 83–106 (1992)
2. Yu, R., Liu, Y., Lu, J.: Design of a TDI CCD data acquisition system. 2012 5th International Conference on BioMedical Engineering and Informatics, pp. 735–738 (2012)
3. Zheng, L., et al.: Noise model of a multispectral TDI CCD imaging system and its parameter estimation of piecewise weighted least square fitting. IEEE Sensor J. 17, 3656–3668 (2017)
4. Cheng, Y., et al.: New on-orbit geometric interior parameters self-calibration approach based on three-view stereoscopic images from high-resolution multi-TDI-CCD optical satellites. Opt. Express. 26, 7475–7493 (2018)
5. Zang, J., et al.: Multi-channel high-speed TDICCD image data acquisition and storage system. 2010 International Conference on E-Product E-Service and E-Entertainment, pp. 1–4 (2010)
6. Shayduk, M., et al.: Fast readout of multi-channel detectors by using a CCD/CMOS camera. IEEE Nuclear Science Symposuim & Medical Imaging Conference, pp. 49–51 (2010)
7. Perry, D.L., Dereniak, E.L.: Linear theory of nonuniformity correction in infrared staring sensors. Opt Eng. 32, 1854–1859 (1993)
8. Yue, J., et al.: Correction of imaging non-uniformity for multi-TDICCD mosaic camera. Optic Precis Eng. 17, 3084–3088 (2009)
9. Liu, Y., Hao, Z.: Research on the nonuniformity correction of linear TDI CCD remote camera. Proc. SPIE. 5633, 527–535 (2005)
10. Yang, J., et al.: Fixed pattern noise pixel-wise linear correction for crime scene imaging CMOS sensor. Proc. SPIE. 10198, 1019802 (2017)
11. Jin, Y., Jiang, J., Zhang, G.: Three-step nonuniformity correction for a highly dynamic intensified charge-coupled device star sensor. Optic. Commun. 285, 1753–1758 (2012)
12. Zhai, G., et al.: The implementation of non-uniformity correction in multi-TDICCD imaging system. Proc SPIE. 9675, 96750A (2015)
13. Wang, Y., Li, C., Lei, N.: Design for the correction system of the real time nonuniformity of large area-array CCD image. Proc SPIE. 8419, 84191R (2012)
14. Zhu, H., et al.: Correction of the non-uniformity for multi-TDICCD mosaic camera on FPGA. 2010 International Conference on E-Product E-Service and E-Entertainment, pp. 1–4 (2010)
15. Shi, C. L., et al.: Two-point multi-section linear nonuniformity correction of IRFPA based on FPGA. Appl. Mech. Mater. 263-266, 3194–3197 (2012)
16. Shi, Y., et al.: A feasible approach for nonuniformity correction in IRFPA with nonlinear response. Infrared Phys. Technol. 46, 329–337 (2005)
17. Sheng, M., Xie, J., Fu, Z.: Calibration-based NUC method in real-time based on IRFPA. Physics Procedia. 22, 372–380 (2011)
18. Zhang, C., Zhao, W.: Scene-based nonuniformity correction using local constant statistics. J. Opt. Soc. Am. A. 25, 1444–1453 (2008)
19. Harris, J.G., Chiang, Y.: Nonuniformity correction of infrared image sequences using the constant-statistics constraint. IEEE Trans. Image Process. 8, 1148–1151 (1999)

20. Liu, Y., Zhu, H., Zhao, Y.: Scene-based nonuniformity correction technique for infrared focal-plane arrays. Appl. Opt. 48, 2364–2372 (2009)
21. Lasarte, M.D., et al.: Optimized algorithm for the spatial nonuniformity correction of an imaging system based on a charge-coupled device color camera. Appl. Opt. 46, 167–174 (2017)
22. Li, H., Man, Y.: Relative radiometric calibration method based on linear CCD imaging the same region of non-uniform scene. Proc. SPIE. 9299, 929906 (2014)
23. Tao, M., Ren, J.: Non-uniformity correction in multi-CCD imaging system. 2010 2nd International Conference on Mechanical and Electronics Engineering. V2, 257–260 (2010)
24. Zhang, G., et al.: On-orbit relative radiometric calibration of the nighttime sensor of the LuoJia1-01 satellite. Sensors. 18, 4225 (2018)
25. Ning, Y., Guo, Y.: Correction of pixel response non-uniformity in TDICCD mosaic camera. Chinese Optics. 6, 386–394 (2013)
26. Chen, N., et al.: Nonuniformity correction for variable-integration-time infrared camera. IEEE Photonics J. 10, 7801611 (2018)
27. LM98640 dual channel, 14-bit, 40 MSPS analog front end with LVDS output technical data Sheet. Texas Instruments (2013)

How to cite this article: Li YH, Wang XD, Wang Z. Compensation for the non-uniformity correction of multi-channel TDI CCD under variable gain. *IET Optoelectron*. 2021;15:27–39. https://doi.org/10.1049/ote2.12011